*Journal of Scientific Computing, Vol. 29, No. 3, December 2006 (© 2005)*
DOI: 10.1007/s10915-005-9016-1

# A Level Set Framework for Capturing Multi-Valued Solutions of Nonlinear First-Order Equations

**Hailiang Liu,[1] Li-Tien Cheng,[2] and Stanley Osher[3]**

*Received December 13, 2004; accepted (in revised form) April 9, 2005; Published online December 7, 2005*

We introduce a level set method for the computation of multi-valued solutions of a general class of nonlinear first-order equations in arbitrary space dimensions. The idea is to realize the solution as well as its gradient as the common zero level set of several level set functions in the jet space. A very generic level set equation for the underlying PDEs is thus derived. Specific forms of the level set equation for both first-order transport equations and first-order Hamilton-Jacobi equations are presented. Using a local level set approach, the multi-valued solutions can be realized numerically as the projection of single-valued solutions of a linear equation in the augmented phase space. The level set approach we use automatically handles these solutions as they appear.

**KEY WORDS:** level set method; multi-valued solutions; nonlinear first-order equations.

**AMS subject classification:** Primary 35F25; Secondary 65M25

## 1. INTRODUCTION

Numerical simulations of high-frequency wave propagation are important in many applications. When the wave field is highly oscillatory in the high-frequency regime, direct numerical simulation of the wave field can be prohibitively costly. Examples include the semiclassical limit for the Schrödinger equation and geometric optics for the wave equation. A natural way to remedy this problem is to use some approximate model which

[1] Mathematics Department, Iowa State University, Ames, IA 50011, USA. E-mail: hliu@iastate.edu
[2] Mathematics Department, UC San Diego, La Jolla, CA 92093-0112, USA. E-mail: lcheng@math.ucsd.edu
[3] Level Set Systems Inc., 1058 Embury Street, Pacific Palisades, CA 90272-2501, USA. E-mail: sjo@levelset.com

can resolve the small-scale in the wave field. The classical approach is the Wentzel–Kramers–Brillonin (WKB) method or geometric optics, which are asymptotic approximations obtained when the small scale becomes finer. Instead of the oscillating wave field, the unknowns in the WKB system are the phase and the amplitude, neither of which depends on the small scale, and typically vary on a much coarser scale than the wave field. Hence they are usually easier to compute numerically.

An obvious drawback of this method is that linear equations are replaced by nonlinear ones, and thereby the superposition principle is lost. In the WKB system the phase is often described by Hamilton-Jacobi (HJ) equations; unfortunately, the classical viscosity solutions [10] are not adequate in describing the superposition nature of waves in phase space. A natural way to avoid such difficulties is to seek multi-valued solutions corresponding to crossing waves. In the last decade, various techniques have been introduced for multi-phase computations found in several applications. Consult [14] for a recent survey on computational high-frequency wave propagation. In [9] we introduced a level set framework to compute the multi-valued solutions to HJ equations, with application to the semiclassical limit of the linear Schrödinger equation.

The goal of our work here is to extend the ideas developed in [9] and [22] for the computation of multi-valued solutions of a very general class of nonlinear first-order equations including $\partial_t S + H(x, S, \nabla_x S) = 0$, to which the previous studies conducted in [9, 22] do not apply. Recently mathematical theory of multi-valued solutions has further been developed in [23], where a notion of geometrical solutions is adopted based on level set formulations introduced in this paper. The well-posedness of the geometrical solutions of HJ equations is established and the relation with entropy and viscosity solutions is clarified.

We begin by sketching the ideas explored in [9], where we focused on the computation of multi-valued solutions of the HJ equation

$$\partial_t S + H(x, \nabla_x S) = 0, \quad x \in \mathbb{R}^n, \tag{1.1}$$

which appears as the phase equation in the semiclassical limit of the linear Schrödinger equation. The level set functions $\phi(t, x, p)$, defined in the phase space $(x, p) \in \mathbb{R}^{2n}$, with $p = \nabla_x S$, each satisfies a linear *Liouville equation*,

$$\partial_t \phi + \nabla_p H \cdot \nabla_x \phi - \nabla_x H \cdot \nabla_p \phi = 0 \tag{1.2}$$

and the multi-valued phase gradient is captured as the intersection of the zero level sets of $n+1$ level set functions (see also [22]). However in the semiclassical regime of the Schrödinger equation, there is also a need to

resolve the multi-valued phase value $S(t, x)$ in the whole domain. In the context of geometric optics, the phase remains constant along the ray [27] (as it does for any Hamiltonian which is homogeneous of degree one in $\nabla S$); the wavefront is therefore defined as the level curve of the phase and the phase solution is completely determined by computing the wavefront location. However in the Schrödinger setting the phase $S$ does change its shape along the ray in $(x, p)$ space. In [9] we defined the wavefront to be the $n-1$ dimensional surface in $(x, p)$ space, driven by the Hamiltonian dynamics (1.2), and starting with a level surface of the initial phase $S_0$. For the computation of such a defined wavefront, we solve $n+1$ decoupled level set equations (1.2), $n$ of these functions can be initialized as the components of $p - \nabla_x S_0$, and the remaining one can be initialized as the level set of the initial phase, e.g., $S_0(x) - C$.

As pointed out in [9], solving the Liouville equation (1.2) alone is not enough to compute the multi-valued phase $S(t, x)$, even on the wavefront described above. Note that in the phase space $(x, p)$, the corresponding phase function $\tilde{S}(t, x, p)$ satisfies a forced hyperbolic transport equation

$$\partial_t \tilde{S} + \nabla_p H \cdot \nabla_x \tilde{S} - \nabla_x H \cdot \nabla_p \tilde{S} = p \cdot \nabla_p H - H. \tag{1.3}$$

The strategy in [9] was to look at the graph of the phase function $z = \tilde{S}(t, x, p)$ in the whole domain, or equivalently to evolve a level set function $\phi = \phi(t, x, p, z)$ in the extended phase space $(x, p, z) \in \mathbb{R}^{2n+1}$

$$\partial_t \phi + \nabla_p H \cdot \nabla_x \phi - \nabla_x H \cdot \nabla_p \phi + (p \cdot \nabla_p H - H)\partial_z \phi = 0. \tag{1.4}$$

In this way, wavefronts with possible multi-phases are tracked and the phase value is numerically resolved via the intersection of $n+1$ zero level sets in the extended space $(x, z, p) \in \mathbb{R}^{2n+1}$ (see e.g. [6, 9]). In particular, the augmented phase space enables us to track the phase $S$ in the entire domain and then project onto the wavefront surface when desired. Note that the Hamiltonian $H$ in (1.1) does not explicitly depend on $S$, and therefore Eq. (1.3) is linear in $S$. Thus, the singularities of $S$ are already 'unfolded' in the phase space $(x, p) \in \mathbb{R}^{2n}$. For this reason, in [9] we chose to either solve the forced Liouville PDE (1.3) in the whole domain or evolve the whole phase as a zero level set in $(x, z, p) \in \mathbb{R}^{2n+1}$, whichever was more convenient. We note that the 'phase space' idea used in [9] is not new and has already been extensively explored in various contexts (see, e.g., [7, 15, 26, 33]). However, the level set equation in the jet space $(x, p, z)$ was formulated for the first time in [9] for HJ equation (1.1). Our aim in this work is to generalize the method in [9] to any first-order PDEs and present some new numerical examples beyond those given in [9].

To put our study in the proper perspective, we recall that there has been a considerable amount of literature available on the computation of multi-valued solutions, ranging from geometric optics [1, 11–13, 27] to the semiclassical regime of Schrödinger equations [9, 17, 21]. In the literature, Lagrangian methods (called ray tracing) and Eulerian methods are the two main approaches used to compute multi-valued solutions. An obvious drawback of the former lies in numerically obtaining adequate spatial resolution of the wavefront in regions with diverging rays. This problem is avoided in Eulerian methods through the use of uniform fixed grids in their computations (see, e.g., [2, 3]). With Eulerian methods, however, difficulties arise in handling the multi-valued solutions that appear beyond singularity formation.

A widely acceptable approach for physical space-based Eulerian methods is the use of a kinetic formulation in the phase space, in terms of a density function that satisfies Liouville's equation, where the technique used to capture multi-valued solutions is based on a closure assumption of a system of equations for the moments of the density (see [4, 5, 12, 16, 17, 21]). In geometric optics and the topic of wavefront construction, geometry-based methods in phase space such as the segment projection method [13], and the level set method [8, 27, 30] have been recently introduced. For the computation of multi-valued solutions to the semiclassical limit of the Schrödinger equation, a new level set method for HJ equations was introduced in [9], to realize the phase $S$ on the whole domain with the level set evolution in an extended space $(x, z, p)$. Furthermore, wavefronts are constructed via the linear *Liouville equation* in the $(x, p)$ space. As remarked earlier our key idea is to build both the 'graph' and the 'gradient' into the zero level set, allowing for computation of multi-valued solutions in the whole domain of physical interest.

Related to our work in [9], on the computation of multi-valued solutions of HJ equation (1.1), is the recent work of [22]. In this paper, the authors used the level set formulation given in [7] to obtain the same result as in this paper for the case of a scalar quasilinear hyperbolic equation. For HJ equations of the type (1.1), where the Hamiltonian does not depend on the solution but only on its gradient, the authors in [22] derived the same level set Liouville equations for the gradient of the phase through an independent approach involving techniques found in [7] and [33]. They presented numerical results in one and two-dimensions that realized the phase gradient for the HJ equation, plotted using the visualization package devised in [24].

In computing the level set equation in phase space, since the area of interest is close to the zero level set, it is possible to use fast local level set techniques in the same manner as in, e.g., [8, 9, 27, 30], which will reduce

the computational cost and (recently) also reduce the storage requirements [25].

This paper is organized as follows. In Sec. 2 we list some nonlinear HJ equations which arise in the high-frequency asymptotic approximation. Section 3 is devoted to a derivation of the generic level set equation for fully nonlinear first-order equations of the form $G(\xi, u, \nabla_\xi u) = 0$. Specific forms of the level set equations for hyperbolic transport equations and HJ equations are presented. Also in this section the computation of multi-valued solutions for several equations are discussed and the required number of level set functions for realizing the solution as well as the choice of corresponding initial data are specified. Finally in Sec. 4 we describe the numerical strategy used and present some numerical results.

## 2. THE WKB METHOD AND HAMILTON-JACOBI EQUATIONS

Before introducing our general level set framework for the computation of multi-valued solutions of first-order PDEs, we pause to consider some applications in high-frequency wave propagations for which we have special HJ equations for the phase function of the wave field. In these cases, the multi-valuedness will reflect the interference of waves. We illustrate as well how nonlinear HJ equations are obtained via the WKB method. Typical applications include the semiclassical limit for Schrödinger equations and geometric optics for the wave equation. The common feature among these problems is the involvement of a small dimensionless parameter $\epsilon$ serving as the microscopic–macroscopic ratio. We look at the $O(\epsilon)$-wave length solutions, which can be tracked in one wave packet with a spatial spreading of the order of $1/\epsilon$ if the initial wave field is highly oscillating and takes the form

$$\psi(x, 0) = A_0(x) \exp(i S_0(x)/\epsilon). \tag{2.1}$$

The usual way to tackle this problem is to use the WKB Ansatz, which consists of representing the wave field function $\psi^\epsilon$ in the form

$$\psi(t, x) = A^\epsilon(t, x) \exp(i S(t, x)/\epsilon). \tag{2.2}$$

With this decomposition, the most singular part of the wave field is characterized by two quantities: the phase function $S$, which satisfies the nonlinear HJ equation, and the amplitude function $A$, which satisfies a transport equation.

The derivation of the WKB system in the linear case is classical (see, e.g., Whitham's book [34]). For linear wave equations subject to highly oscillatory initial data, insertion of (2.2) into the underlying equations

leads to corresponding relations between the wave's phase $S$ and its amplitude. Splitting the relation into real and imaginary parts and taking the lowest-order (in terms of $\epsilon$) terms, one often obtains weakly coupled WKB systems of the form

$$\partial_t S + H(x, \nabla_x S) = 0,$$
$$\partial_t \rho + \nabla_x \cdot (\rho \nabla_p H(x, \nabla_x S)) = 0,$$

where $\rho$ is related to the amplitude $A$. We list here two examples, see [32] for more WKB-systems derived from generalized dispersive equations.

(1) Linear Schrödinger equation:

$$i\epsilon \partial_t \psi^\epsilon = -\frac{\epsilon^2}{2} \Delta \psi^\epsilon + V(x)\psi^\epsilon, \quad x \in \mathbb{R}^d \tag{2.3}$$

where $V$ is the corresponding potential, and $\epsilon$ the scaled Planck constant. In this case $H(x, p) = \frac{|p|^2}{2} + V(x)$ and $\rho = A^2$.

(2) The wave equation in an inhomogeneous medium with a variable local speed $c(x)$ of wave propagation in the medium:

$$\partial_t^2 \psi^\epsilon = c^2(x) \Delta \psi^\epsilon, \quad x \in \mathbb{R}^d \tag{2.4}$$

for which we have $H(x, p) = c(x)|p|$ and $\rho = A^2/c(x)$.

We note that for the wave equation (2.4), if we look for a planar wave solution $\psi = u(x)\exp(it/\epsilon)$, we are led to a steady state function solving the scalar Helmholtz equation

$$-(\Delta + k^2)u = 0, \quad k := (\epsilon c(x))^{-1}. \tag{2.5}$$

Searching for solutions oscillating with frequency $1/\epsilon$, we could use the ansatz $u(x) = A(x)\exp(iS(x)/\epsilon)$, leading to a weakly coupled system,

$$c(x)|\nabla_x S| = 1, \quad \nabla_x \cdot (A^2 \nabla_x S) = 0. \tag{2.6}$$

In the paraxial application, one spatial variable is regarded as the evolution direction and the above steady eikonal equation may be written as

$$\partial_{x_2} S - \sqrt{c^{-2} - (\partial_{x_1} S)^2} = 0$$

or a variant of this (see e.g. [18]). This is again a 'time-dependent' HJ equation. From the above weakly coupled systems we see that the multi-valued phase $S$ can be computed from the nonlinear HJ equations, independent of amplitude, and the amplitude is forced to become multi-valued at points where the phase is multi-valued.

## 3. LEVEL SET EVOLUTION

Consider a general first-order nonlinear equation

$$G(\xi, u, \nabla_\xi u) = 0, \tag{3.1}$$

where $u \in \mathbb{R}^1$ is a scalar unknown and $\xi \in \mathbb{R}^m$ is the independent variable. Furthermore, $G = G(\xi, z, q)$, $(\xi, z, q) \in \mathbb{R}^{2m+1}$ is a given function satisfying the nondegeneracy assumption

$$|\nabla_q G(\xi, z, q)|^2 \neq 0,$$

which ensures that (3.1) is, in fact, a first-order equation.

In order to visualize the solution profile (single-valued or multi-valued), following [9], we introduce a generic level set function $\phi(\xi, z, q)$ in an extended space $(\xi, z, q) \in \mathbb{R}^{2m+1}$ so that the solution $z = u(\xi)$, and also its gradient $\nabla_\xi u$, stay on the zero level set

$$\phi(\xi, z, q) = 0, \quad z = u(\xi), \quad q = \nabla_\xi u(\xi).$$

Since Eq. (3.1) is a first-order equation, its characteristics exist at least locally. Let such characteristics be parameterized as $(\xi, z, q) = (\xi, z, q)(\tau)$. The level set function should be independent of the parameter $\tau$. Therefore,

$$\frac{d}{d\tau}\phi(\xi(\tau), z(\tau), q(\tau)) \equiv 0,$$

which gives the level set equation

$$\vec{A} \cdot \nabla_{\{\xi, z, q\}} \phi = 0,$$

where $\vec{A} := (\frac{d\xi}{d\tau}, \frac{dz}{d\tau}, \frac{dq}{d\tau})$ denotes the direction field of the characteristics. According to the classical theory of characteristics for general differential equations of the first order, see [7, pp. 142–144], the vector field is obtained as

$$A_1 = \nabla_q G, \quad A_2 = q \cdot \nabla_q G, \quad A_3 = -\nabla_\xi G - q \cdot \partial_z G.$$

Thus our level set equation is

$$\nabla_q G \cdot \nabla_\xi \phi + q \cdot \nabla_q G \partial_z \phi - (\nabla_\xi G + q \partial_z G) \cdot \nabla_q \phi = 0, \tag{3.2}$$

which as a linear equation serves to 'unfold' multi-valued quantities wherever they occur in the physical space. The level set equation in such generality can be used to capture wavefronts, and to recover the solution value $u$ and the gradient of the solution when desired.

Based on the general level set equation (3.2), we can write down the corresponding form of the level set equation once the target PDE is given. To implement the level set method for a given problem we still need to further check (i) whether reducing to a lower dimension is possible (to reduce computational cost); (ii) how many level set functions are needed; and (iii) how the initial data is chosen. Here are some guiding principles:

- When implementing the level set method, reducing to a lower dimension is preferred for lowering the computational cost. In general such reduction is indeed possible if the variables in the lower dimension give us the quantities we want to compute and these variables evolve along the characteristic field independent of other variables in the full space $(\xi, z, q)$.
- If the reduced space dimension is $m$ and the object of interest is $k$ dimensional, then use $m-k$ level set functions;
- The initial data should be chosen in such a way that the intersection of zero level sets of these chosen initial data uniquely embeds the given initial data in the original PDE problem.

The level set method has proven to be a powerful tool for capturing the dynamic evolution of surfaces (see [28, 29]). We now demonstrate the level set method by looking at hyperbolic transport equations and HJ equations, which are two prototypical examples of first-order PDEs. We will study how many level set functions are needed to determine the desired quantities, and how to choose initial data to generate these level set functions.

### 3.1. Hyperbolic Transport Equations

Consider the first-order time-dependent transport equation:

$$\partial_t u + F(u, x, t) \cdot \nabla_x u = B(u, x, t), \quad x \in \mathbb{R}^n, \quad u \in \mathbb{R}^1 \tag{3.3}$$

subject to smooth initial data $u(0, x) = u_0(x)$.

Take $\xi = (t, x)$ and $q = (p_0, p)$ with $p_0 = \partial_t u$, $p := \nabla_x u$, and Eq. (3.3) can be rewritten as $G = 0$ where

$$G := p_0 + F(z, x, t) \cdot p - B(z, x, t), \quad z = u.$$

A simple calculation gives

$$\nabla_q G \cdot \nabla_\xi \phi = \partial_t \phi + F(z, x, t) \cdot \nabla_x \phi$$

and

$$q \cdot \nabla_q G\phi_z = (1, F) \cdot (p_0, p) = p_0 + F \cdot p = B(z, x, t)\phi_z,$$

where we have used the fact $G = p_0 + F \cdot p - B = 0$. The level set equation (3.2) in this setting reduces to

$$\partial_t \phi + F \cdot \nabla_x \phi + B\partial_z \phi + A_3 \cdot \nabla_q \phi = 0.$$

Note that the transport speeds in the $x$ and $z$-directions do not explicitly depend on $(p_0, p)$. Therefore, the level set function will not depend on $q = (p_0, p)$ if it does not do so initially. Thus, the effective level set equation in the phase space $(t, x, z)$ reads as

$$\partial_t \phi + F \cdot \nabla_x \phi + B\partial_z \phi = 0. \tag{3.4}$$

The solution $u$ to (3.3) with initial data $u(0, x) = u_0(x)$ can be determined as the zero level set,

$$\phi(t, x, z) = 0, \quad z = u(x, t).$$

In this case, we only need one level set function $\phi$. The initial data can simply be chosen as

$$\phi(0, x, z) = z - u_0(x)$$

or alternatively the signed distance to the surface $z = u_0(x)$ in the case of nonsmooth data. Here the zero level set $\phi(t, x, u) = 0$ can be regarded as a complete integral to (3.4), which implicitly determines $u$ (see [7, p. 140]).

### 3.2. Generalized Hamilton-Jacobi Equations

Consider a generalized HJ equation

$$\partial_t S + H(x, S, \nabla_x S) = 0 \tag{3.5}$$

subject to the initial data

$$S(x, 0) = S_0(x), \quad x \in \mathbb{R}^n. \tag{3.6}$$

Note, in previous literature, e.g. [10], this equation was simply referred to as HJ equation. Here, we call it generalized HJ equation to distinguish it from the case where the Hamiltonian does not depend on $S$ explicitly. The inclusion of $S$ fundamentally changes the behavior of the solution. Thus, the previous studies conducted in [9] do not apply in this situation.

Taking $\xi = (t, x)$ and $q = (p_0, p)$ with $p_0 = \partial_t S, \quad p = \nabla_x S$, Eq. (3.5) can be rewritten as $G = 0$, where

$$G := p_0 + H(x, z, p), \quad z = S.$$

A straightforward calculation gives

$$\begin{aligned} \partial_q G \cdot \nabla_\xi \phi &= \partial_t \phi + \nabla_p H \cdot \nabla_x \phi, \\ q \cdot \nabla_q G \partial_z \phi &= (p \cdot \nabla_p H - H) \partial_z \phi \end{aligned}$$

and

$$\nabla_\xi G + q \cdot \partial_z G = (0, \nabla_x H) + (p_0, p) H_z = (-H H_z, \nabla_x H + p H_z),$$

where we have used $p_0 = -H(x, z, p)$. The level set equation in the full phase space $(x, z, p, p_0)$ thus becomes

$$\partial_t \phi + \nabla_p H \cdot \nabla_x \phi + (p \cdot \nabla_p H - H) \partial_z \phi - (\nabla_x H + p H_z) \nabla_p \phi + H H_z \partial_{p_0} \phi = 0.$$

The effective level set equation for (3.5), when capturing $p_0 = \partial_t S$ is not a goal, yields

$$\partial_t \phi + \nabla_p H \cdot \nabla_x \phi + (p \cdot \nabla_p H - H) \partial_z \phi - (\nabla_x H + p H_z) \nabla_p \phi = 0, \tag{3.7}$$

where $\phi := \phi(t, x, z, p)$ is well defined in the space $(x, z, p) \in \mathbb{R}^{2n+1}$ for fixed $t$. The solution $S$ is evolved as the zero level set of $\phi = \phi(t, x, z, p)$ with $z = S, \quad p = \nabla_x S$,

Since $(p, z) \in \mathbb{R}^{n+1}$, we need $(n+1)$ level set functions $\phi_i(t, x, z, p) (i = 1, \ldots, n+1)$ in this case. Their common zero level set captures the desired solution $z = S$ in the jet space $(x, p, z)$. As a by-product, the multi-valued $p = \nabla_x S$ will also be determined in this procedure.

For these level set functions, the corresponding initial data can be simply chosen as

$$\phi_1(0, x, z, p) = z - S_0(x), \tag{3.8}$$

$$\phi_i(0, x, z, p) = p_i - \partial_{x_i} S_0(x), \quad i = 2, \ldots, n+1. \tag{3.9}$$

Again for nonsmooth data, we need to use instead the signed distance function to the surfaces $z = S_0(x)$ or $p = \nabla_x S_0(x)$.

If the Hamiltonian $H$ does not depend explicitly on $S$, i.e., $H_z = 0$, (3.7) will lead to the level set equation

$$\partial_t \phi + \nabla_p H \cdot \nabla_x \phi + (p \cdot \nabla_p H - H) \partial_z \phi - \nabla_x H \nabla_p \phi = 0. \tag{3.10}$$

Note that when $H$ does not depend on $z$ explicitly, the level set function $\phi$ will be independent of $z$, if it is chosen so initially. Therefore, if one just wants to capture the wavefront or resolve the gradient of $S$, the effective level set equation reduces to

$$\partial_t \phi + \nabla_p H \cdot \nabla_x \phi - \nabla_x H \cdot \nabla_p \phi = 0.$$

This is the well-known Liouville equation (1.2). In this case, only $n$ independent level set functions are needed for capturing the phase gradient $\nabla_x S$ (see [9, 22]).

## 4. NUMERICAL TESTS

The level set equation for first-order time-dependent PDEs takes the form

$$\partial_t \phi + \vec{A}(X) \cdot \nabla_X \phi = 0 \tag{4.1}$$

with $X = (x, z, p)$ being the variable in the extended phase space and the coefficient $\vec{A}(X)$ depending on the phase variable $X$. We apply variants of the numerical algorithm developed in [9] to (4.1) to capture possible multi-valued solutions of the original nonlinear PDEs.

We conclude the paper with a number of numerical examples. We present mainly 1D examples focusing on the computation of phase in the whole domain; consult [9] for phase computations restricted on wavefronts and [22] for the computation of phase gradient (velocity). The details of the level set algorithms, including boundary conditions, grid sizes, and time steps used, and the intricacies of reinitialization, following the numerical studies of [9].

### 4.1. One-Dimensional Transport Equations

Consider the scalar transport equation

$$\partial_t u + \partial_x f(u) = -v'(x), \quad x \in \mathbb{R}$$

subject to the initial data $u(x, 0) = u_0(x)$. Usually of interest is the viscosity solution of this PDE satisyfing the entropy condition. However, we are interested here in the calculation of multi-valued solutions. Our level set approach, in this case, realizes this type of solution as the zero level set

$$\phi(t, x, z) = 0, \quad z = u(x, t)$$

evolving with the level set function $\phi$ under the transport equation

$$\partial_t \phi + f'(z)\partial_x \phi - v'(x)\partial_z \phi = 0.$$

Initial data for this equation is chosen to satisfy $z = u_0(x)$, and thus one common choice is

$$\phi_0(x) = z - u_0(x).$$

**Example 1—Inviscid Burgers' Equation**

Consider the inviscid Burgers' equation

$$\partial_t u + \partial_x \left[ \frac{u^2}{2} \right] = 0$$

with smooth periodic initial data

$$u_0(x) = 0.5 + \sin(x).$$

The solution of this PDE is well-analyzed, and we know that it develops a singularity at the critical time $T_c = 1$ and spatial location $x = (2k+1)\pi + 0.5$, for each $k \in \mathbb{Z}$.

The PDE for evolution of $\phi$ takes the form

$$\partial_t \phi + z\partial_x \phi = 0,$$

with initial data

$$\phi_0(x) = z - (0.5 + \sin(x)).$$

Figure 1 shows the behavior of the multi-valued solution computed using our algorithm. The zero level sets of $\phi$ at different times are plotted in the same graph. Notice we are able to capture the overturning of the function at the correct location $x = -\pi + 0.5$. This overturning is a shock in the standard entropy solution.

**Example 2—Nonconvex Flux**

Consider the Riemann problem

$$\partial_t u + \partial_x \left[ \frac{(u^2-1)(u^2-4)}{4} \right] = 0$$

with discontinuous initial data

$$u_0(x) = \begin{cases} 2, & x \le 0, \\ -2, & x > 0. \end{cases}$$

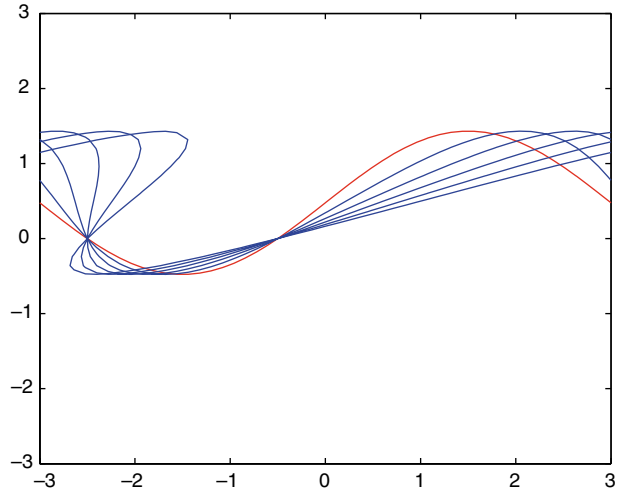


**Fig. 1.** Our approach capturing an initial sine function overturning to become multi-valued. The plots are at 0.3921268 time intervals, with the final curve at time 1.96063.

Thus the initial data has a discontinuity at $x = 0$ which overturns at later time.

In this case, the level set evolution equation takes the form

$$\partial_t \phi + z\left(z^2 - \frac{5}{2}\right)\partial_x \phi = 0$$

and we choose $\phi_0(x)$ to be the signed distance function associated to the graph of $u_0(x)$, due to the discontinuity. Figure 2 shows the multi-valued solution associated to this problem. We plot in the same graph the time evolution, in equal time intervals, of the initial function using our algorithm. Overturning is clearly seen and there are up to five values of the function at a given $x$. Our approach is able to capture all of the multi-valued phenomena.

### 4.2. One-Dimensional Hamilton-Jacobi Equations

Consider the HJ equation

$$\partial_t S + \frac{1}{2}|\partial_x S|^2 + V(x) = 0,$$

where $V(x)$ is a function called the potential. Furthermore, let $S_0(x)$ be the initial data for $S$. This specific set of equations arises as the semiclassical limit of the linear Schrödinger equation, where $S$ denotes the phase (see, e.g., [9, 21, 32]).

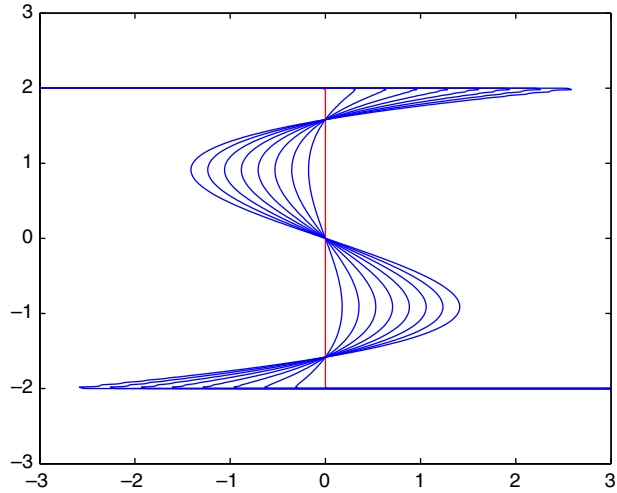


**Fig. 2.** Our approach applied to a Riemann problem, with initial step function, that produces multi-valued solutions. The plots are at 0.1160138 time intervals with the final curve at time 0.928111.

**Example 3—Free motion $V \equiv 0$**

In the case of free motion, where $V \equiv 0$, the HJ equation reduces to

$$\partial_t S + \tfrac{1}{2}|\partial_x S|^2 = 0.$$

In our level set approach, we introduce the two component vector valued level set function $\phi = \phi(t, x, z, p)$, which satisfies the equation for motion,

$$\partial_t \phi + p\partial_x \phi + \frac{p^2}{2}\partial_z \phi = 0.$$

Furthermore, we can in many cases take as initial data for $\phi$,

$$\phi_1(0) = z - S_0(x), \qquad \phi_2(0) = p - \partial_x S_0(x),$$

where $\phi_1$ and $\phi_2$ denote the first and second components of $\phi$, respectively.

The specific cases we consider are:

(1) **Case—No caustic**

$$S_0(x) = \frac{x^2}{2}, \quad x \in \mathbb{R}.$$

In this case, the solution $S$ remains smooth for all time, taking the form

$$S(x,t)=\frac{x^2}{2(t+1)}.$$

Figure 3 shows the results of our algorithm in $xz$-space, projecting away $p$, on this problem. The initial parabola flattens out as time increases but no multi-valuedness occurs.

(2) **Case—Focusing at a Point**

$$S_0(x)=-\frac{x^2}{2},\quad x\in\mathbb{R}.$$

In this case, all rays intersect at the focus point $(x,T_c)=(0,1)$, and then spread out afterwards. Thus almost everywhere in space, there is a single-valued phase, taking the form

$$S(x,t)=\frac{x^2}{2(t-1)}.$$

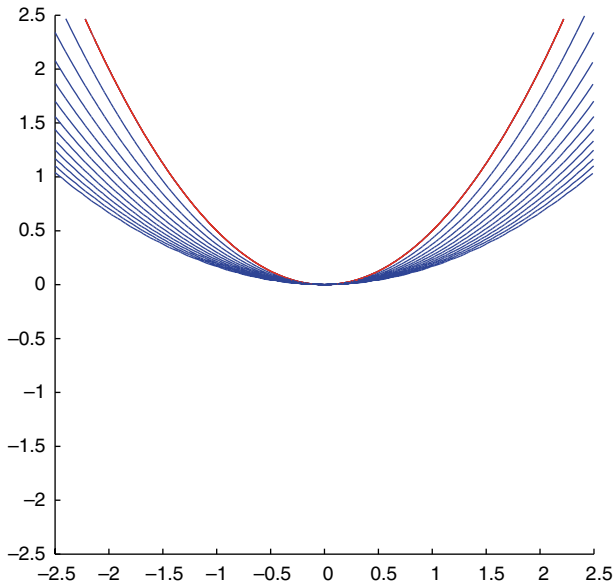


**Fig. 3.** Our approach for free motion on an initial parabola, the one above the rest. No singularities appear in this example. The plots are at time intervals of 0.167318 with the final curve at time 2.00781.

Figure 4 shows our projected results in $xz$-space for this example. The initially inverted parabola becomes thinner and thinner, eventually flipping over to parabolas lying above the $x$-axis and expanding. Some of the parabolas are "cut off" in the graph due to the finite $z$-direction of the domain used in our computations.

(3) **Case—Caustic**

$$S_0(x) = -\ln(\cosh(x)), \quad x \in \mathbb{R}.$$

In this case, a singularity appears at time 1 and located at $x = 0$. After this time and from this location, a multi-valued phase appears. Figure 5 shows the behavior of the solution obtained from our algorithm plotted at equal time intervals up to time 1.5. The shrinking solutions develop a swallow-tail singularity after the critical time $T_c = 1$ at $x = 0$. A zoom of specifically this multi-valuedness between time 1 and 1.5 are also shown in the figure. These results fit with the analysis of the PDE.

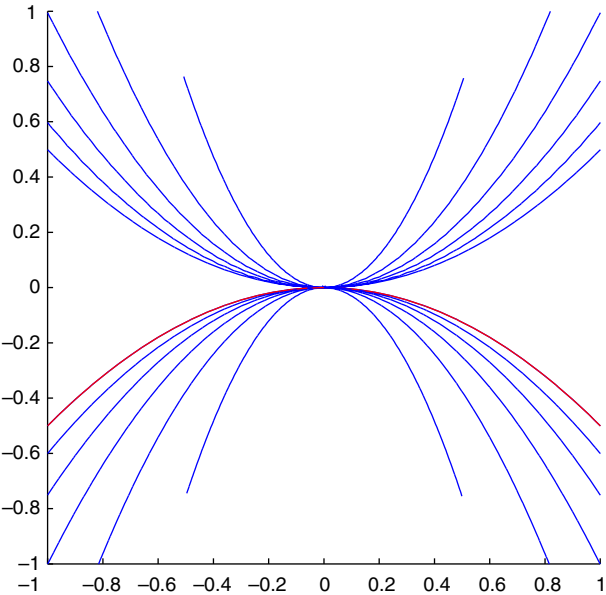


**Fig. 4.** Our approach showing focusing on an initial inverted parabola, the uppermost concave down one. The parabola remains concave down and adds curvature before the singularity, afterwhich it switches to concave up and relaxing in curvature. The plots are at time intervals of 0.1669248 with the final curve at time 2.0031.

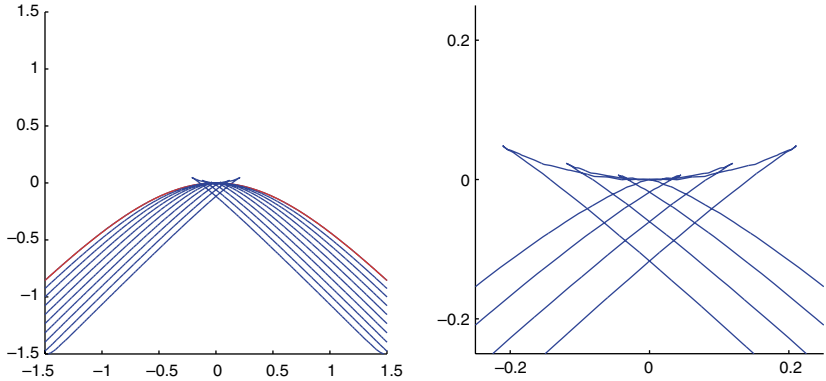


**Fig. 5.** Our approach capturing caustics, with a swallow-tail multi-valuedness developing at the critical time with initial curve the uppermost concave down parabola. The plots are at time intervals of 0.1673176 with the final curve at time 1.50586. The figure on the right is a zoomed picture around the singularity of the solutions at and after the critical time.

### Example 4—Harmonic oscillator $V(x)=x^2/2$

For general $V(x)$, the level set evolution equation takes the form

$$\partial_t\phi + p\partial_x\phi + \left(\frac{p^2}{2} - V(x)\right)\partial_z\phi - \partial_x V(x)\partial_p\phi = 0$$

and the initial data can in many cases be taken as

$$\phi_1(0) = z - S_0(x), \quad \phi_2(0) = p - \partial_x S_0(x).$$

For $V(x)=x^2/2$ and $S_0(x)=x$ (see [32]), rays will intersect at the focal points

$$(x, T_c) = \left((-1)^{m+1}, \frac{(2m+1)\pi}{2}\right), \quad m \in \mathbb{Z}.$$

The solution in fact is explicitly given as

$$S(x,t) = -\frac{1}{2}(x^2+1)\tan(t) + \frac{x}{\cos(t)}, \quad t \neq \frac{(2m+1)\pi}{2}.$$

Figure 6 shows our results, plotted in $xz$-space, for this problem. The initial line $z=x$ first focuses at $x=1$ and then subsequently at $x=-1$, at each time developing multi-valuedness after the focusing. This oscillation continues since the singularties form periodic in time. Although there are once

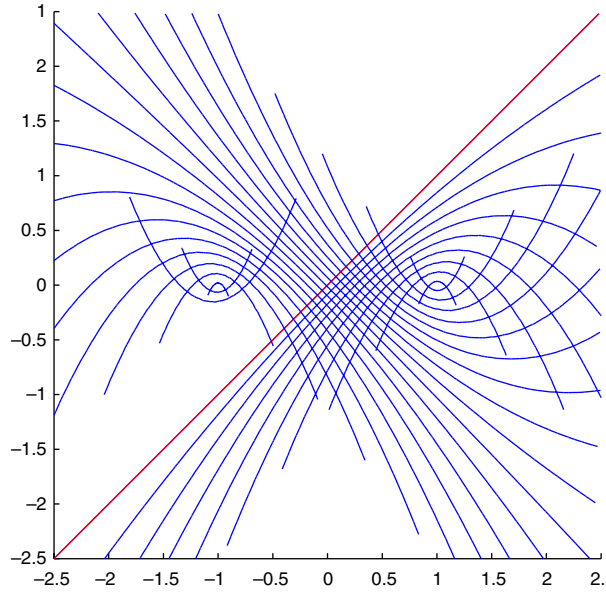


**Fig. 6.** Our approach for the harmonic oscillator showing oscillating focusing effects occuring between two points. The inital curve is the line through the origin of slope 1. This subsequently bends into concave down parabolas, then concave up ones about the singularity on the right. In later time these straighten out to a line of slope $-1$ and reproduce the behavior about the singularity on the left. The plots are at time intervals of 0.333484 with the final curve at time 10.0045.

again "cut offs" due to the computational domain used, we are still able to capture the multi-valued solution throughout the focusing effects.

**Example 6—Other multi-valued phenomena**

In the semiclassical limit for plasma, there appears the equation

$$S_t + \frac{|S_x|^2}{2} = -\alpha S$$

with $S_0(x) = -|x|$ and some physical parameter $\alpha > 0$. With $x \in \mathbb{R}^1$ and $\alpha = 1$, we plot the results in Fig. 7 along with branches of the exact solution at the final time. These branches satisfy $-(|x| + t)e^{-t} + 0.5(1 - e^{-t})$ for $|x| > t$, and $(\pm|x| - t)e^{-t} + 0.5(1 - e^{-t})$ or $0.5x^2(1 - e^{-t})/t^2$ for $|x| \leq t$. The multi-valued characteristics match and the positions are in good agreement except for the small, thin loops at the ends of the swallow-tails, whose lengths are cut by half in the computed solution. This may be due to numerical diffusion and resolution with the nonsmooth initial data.

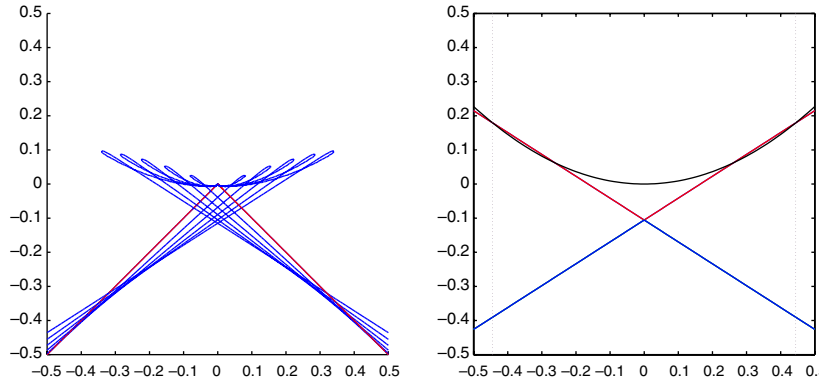


**Fig. 7.** Our approach applied in the semiclassical limit for plasma is shown. The initial curve, the inverted V-shape, develops a swallow-tail with small, thin loops at the ends. The plots are at time intervals of 0.888888 with the final curve at time 0.444444. The figure on the right shows branches of the exact solution with the same characteristics as in the computed solution.

## ACKNOWLEDGMENTS

Liu's research was supported in part by the National Science Foundation under Grant DMS05-05975, Cheng's research was supported in part by NSF grant #0208449 and Osher's research was supported by AFOSR Grant F49620-01-1-0189.

## REFERENCES

1. Benamou, J. D., Castella, F., Katsaounis T., and Perthame, B. (2001). *High-frequency Helmholtz Equation, Geometrical Optics and Particle Methods*, Revist. Math. Iberoam.
2. Benamou, J.-D. (1996). Big ray tracing: multivalued travel time field computation using viscosity solution of the eikonal equation. *J. Comp. Phys.*, **128**, 463–474.
3. Benamou, J. D. (1999). Direct solution of multivalued phase space solutions for Hamilton-Jacobi equations. *Comm. Pure Appl. math.*, **52**, 1443–1475.
4. Brenier, Y. (1984). Averaged multivalued solutions for scalar conservation laws. *SIAM J. Numer. Anal*. **21**, 1013–1037.
5. Brenier, Y., and Corrias, L. (1998). A kinetic formulation for multi-branch entropy solutions of scalar conservation laws. *Ann. Inst. Henri Poincare* **15**, 169–190.
6. Burchard, P., Cheng, L.-T., Merriman, B., and Osher, S. (2001). Motion of curves in three spatial dimensions using a level set approach. *J. Comput. Phys*. **170**, 720–741.
7. Courant, R,. and Hilbert, D. (1952–1962). *Methods of Mathematical Physics*, Vol 2, Interscience Publishers, New York.
8. Cheng, L.-T., Osher, S., Kang, M., Shim, H., and Tsai, Y.-H. Reflection in a level set framework for geometric optics. *Comp. Methods Eng. Phys*. to appear.
9. Cheng, L.-T., Liu, H.-L., and Osher, S. (2003). Computational high-frequency wave propagation in Schödinger equations using the Level Set Method, with applications to the semi-classical limit of Schrödinger equations. *Comm. Math. Sci*. **1**(3), 593–621.

10. Crandall, M., and Lions, P. L. (1984). Viscosity solutions of Hamilton-Jacobi equations. *Trans. AM. Math. Soc*. **282**, 487.
11. Engquist, B., Fatemi, E., and Osher, S. (1995). Numerical solution of the high frequency asymptotic expansion for the scalar wave equation. *J. Comput. Phys.* **120**, 145–155.
12. Engquist, B., and Runborg, O. (1996). Multi-phase computations in geometrical optics *J. Comp. Appl. Math.* **74**, 175–1992.
13. Engquist, B., Runborg, O. and Tornberg, T.-K. (2002). High frequency wave propagation by the segment projection method. *J. Comput. Phys*. **178**, 373–390.
14. Engquist, B., and Runborg, O. (2003). Computational high frequency wave propagation, Acta Numerica, 2003.
15. Evans, L.-C. (1996). A geometric interpretation of the heat equation with multi-valued initial data. *SIAM J. Math. Anal*. **27**, 932–958.
16. Gosse, L. (2002). Using K-branch entropy solutions for multivalued geometric optics computations. *J. Comp. Phys.*, **180**, 155–182.
17. Gosse, L., Jin, S., and Li, X. (2003). On two moment systems for computing multiphase semiclassical limits of the Schrödinger equation. *Math. Models Methods Appl. Sci*. **13**(12), 1689–1723.
18. Gray, S., and May, W. (1994). Kirchhoff migration using eikonal equation travel times. *Geophysics*, **59**, 810–817.
19. Gasser, I., and Markowich, P. A. (1997). Quantum hydrodynamics, Wigner transform and the classical limit. *Asymptotic Anal*. **14**, 97–116.
20. Gerard, P., Markowich, P. A., Mauser, N. J., and Poupaud, F. (1997). Homogenization limits and Wigner transforms. *Comm. Pure Appl. Math*. **50**, 323–380.
21. Jin, S., and X. Li, Multi-phase computations of the semiclassical limit of the Schrödinger equation and related problems: Whitham vs Wigner. *Physics D.* **182** (2003), no. (1–2), 46–85.
22. Jin, S., and Osher, S. A level set method for the computation of multivalued solutions to quasi-linear hyperbolic PDE's and Hamilton-Jacobi equations. submitted to Comm. Math. Sci.
23. Liu, H. Geometrical solutions of Hamilton-Jacobi equations, preprint (2004).
24. Min, C. (2003). Simplicial isosurfacing in arbitrary dimension and codimension. *J. Comput. Phys*. **190**, 295–310.
25. Min, C. (2004). Local level set method in high dimension and codimension. *J. Comput. Phys*. **200**, 368–382.
26. Osher, S. (1993). A level set formulation for the solution of the Dirichlet problem for Hamilton-Jacobi equations. *SIAM J. Math. Anal*. **24**, 1145–1152.
27. Osher, S., Cheng, L.-T., Kang, M., Shim, H., and Tsai, Y.-H. (2002). Geometric optics in a phase space based level set and eulerian framework. *J. Comput. Phys*. **179**, 622–648.
28. Osher, S., and Fedkiw, R., *Level Set Method and Dynamic Implicit Surfaces*. Springer-Verlag, NY.
29. Osher, S., and Sethian, J. (1988). Fronts propagating with curvature dependent speed: algorithms based on Hamilton-Jacobi formulations. *J. Comput. Phys*. **79**, 12–49.
30. Qian, J., Cheng, L.-T., and Osher, S. (2003). A level set based Eulerian approach for anisotropic wave propagation. *Wave Motion* **37**, 365–379.
31. Runborg, O. (2000). Some new results in multi-phase geometric optics. *Math. Model. Num. Anal.* **34**, 1203–1231.
32. Sparber, C., Markowich, P. A., and Mauser, N. J. (2003). Wigner functions versus WKB-methods in multivalued geometrical optics. *Asymptot. Anal*. **33**(2), 153–187.

33. Tsai, Y.-H. R., Giga, Y., and Osher, S. (2003). A level set approach for computing discontinuous solutions of Hamilton-Jacobi equations. *Math. Comp.* **72**, 159–181.
34. Whitham, G. B. (1974). *Linear and Nonlinear Waves*, Wiley-Interscience [John Wiley & Sons], New York.